Analysis for surface probes prepared 10th experimental campaign of LHD

H. Yagihashi[a], T. Hirata[a], N. Ashikawa[b], T. Hino[a],
Y. Yamauchi[a], Y. Nobuta[a], S. Masuzaki[b], K. Nishimura[b],
A. Sagara[b], N. Oyabu[b], A. Komori[b], O. Motojima[b]

[1]*Laboratory of Plasma Physics and Engineering, Hokkaido University, Kita-13, Nishi-8, Kita-ku, Sapporo, 060-8628, Japan*
[2]*National Institute of Fusion Science, Oroshi-cho, Toki, Gifu, Japan*

(Received: 3 September 2008 / Accepted: 5 January 2009)

Abstract

The characteristics of deposition/erosion and the gas retention on the sample probes were investigated in the Large Helical Device (LHD). Major species of deposits were carbon, boron, oxygen and iron. The carbon was observed on the top surface layer and the thickness of this layer was 40-80 nm with the concentration of 80-90 at%. The amount of retained hydrogen and helium were relatively large near the anodes during H_2 and He glow discharge. The helium retention was large near the ICRF antenna due to the influence by high energy helium ions heated by ICRF heating. The amount of retained helium was one order smaller than that of hydrogen. These results contribute to understanding the plasma wall interaction in LHD.

Keywords: LHD; Material probe; Gas retention; Boronization; erosion

1. Introduction

It is quite important to know the wall conditions in fusion devices and plasma surface interactions arising from the progress of plasma experiments. For this reason, the wall condition data have been systematically accumulated from the 1st experimental campaigns (1998) of the large helical device (LHD). The results for the campaign from 1998 to 2005 were reported in previous papers [1- 6].

This paper presents the results obtained in the 10th experimental campaign (2006-2007) in the LHD using sample probes. The deposits and the retained amounts of discharge gases and impurity gases on these probes were examined by Auger electron spectroscopy (AES) and thermal desorption spectroscopy (TDS), respectively. In addition, the sample probes with pre-coated boron film were also exposed to the plasma to estimate the erosion during one experimental campaign.

2. Experimental

In the LHD, the first wall and the divertor target tiles were made of 316L stainless steel (SS316L) and graphite, respectively. The area of the inner wall was 780m^2. In the 10th experimental campaign, the total shot number of main discharges was 7800; 5500 shots of H_2 discharges and 2300 of He discharges. The glow discharge cleaning (GDC) was conducted for totally 740h; 260h with H_2, 400h with He, 60h with Ne, 20h with Ar. Boronizations using glow discharge with a mixtured gas of helium (90%) and diborane (10%) were conducted twice during the campaign [1-2].

The sample probes were placed at the bottom side on the horizontally elongated cross-section.in each toroidal sector as shown in Fig.1. Both SS316L and silicon (Si) probes were set in each sample holder. The size of each probe was 10mm × 20mm and thickness is 1mm. In order to estimate the erosion depth, boron film was pre-coated on one half area of silicon probe. Two anodes were located at the 4.5 and 10.5U ports, and the diborane-inlet nozzles were located at the 1.5, 3.5 and 7.5 ports. These positions are also shown in Fig.1.

Three kinds of heating system are operated in LHD. They are electron cyclotron heating (ECH), four neutral beam injectors (NBI) and the ion cyclotron range of frequency (ICRF) heating systems. The ICRF system is mainly developed to supported long pulse discharge plasmas [7].

The eroded depth was derived from the following way. The depth profile of Si probe and pre-coated boron Si probe (B/Si probe) were examined by using AES. A same thickness of impurity layer was deposited on the top surface of Si probe and B/Si probe. Subtract the thickness of impurity layer from the whole thickness of B/Si depth profile. This value is corresponding to remained

E-mail address: yagiha@pop.qe.eng.hokudai.ac.jp

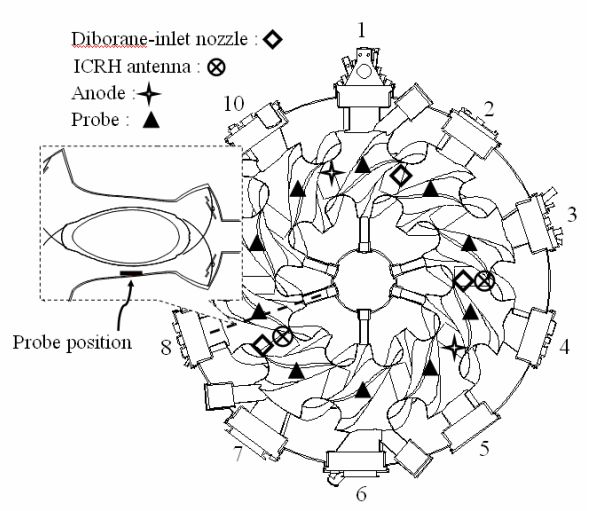

Fig.1 Toroidal locations of material probes and diborane-inlet nozzles, ICRH antennae, anodes, NBI direction.

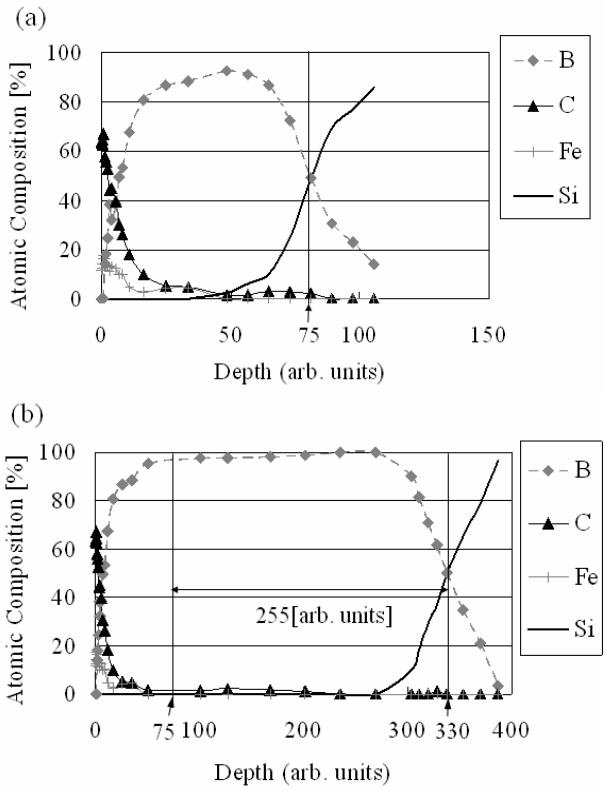

Fig.2 The depth profiles of the atomic compositions on the surface of the sample probes at sector 7. (a) Si sample, (b) Si sample with pre-coated B.

pre-coated boron film on the Si substrate, did not eroded by plasma. The net eroded depth was obtained by subtracting this remained boron film thickness from the known pre-coated boron film thickness. Here, conversion factor of AES result to the real depth is 2/3. Therefore, the thickness of 75 (a.u.) by AES corresponds to the real thickness of 50 nm (75×2/3).

In Fig. 2, the thickness of deposition layer on Si probe was 75(a.u.) (Fig. 2 (a)) and that of B/Si probe was 330(a.u.)

E-mail address: yagiha@pop.qe.eng.hokudai.ac.jp

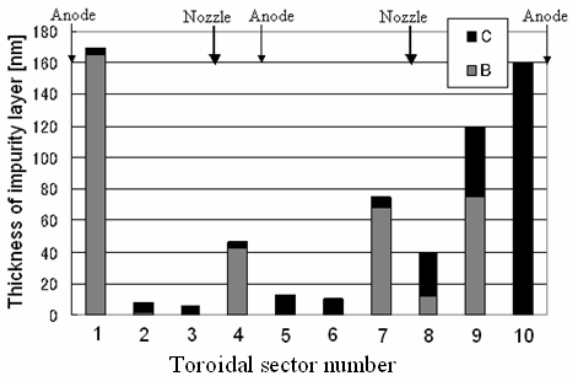

Fig.3 Thickness of impurity layer vs toroidal sector number.

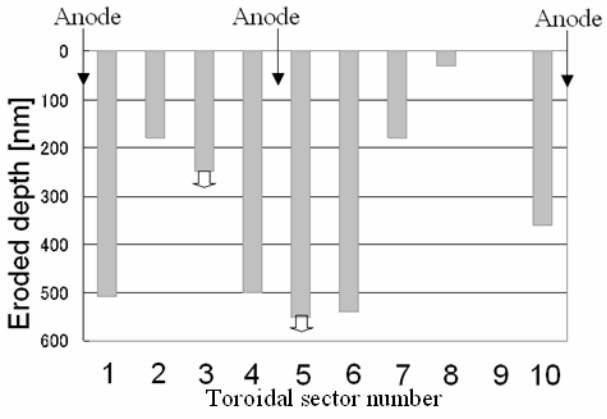

Fig.4 Eroded depth of pre-coated boron film vs toroidal sector number.

(Fig. 2 (b)) in sector 7. The remained pre-coated boron film was 255(a.u) (330 – 75). Then the actual thickness of remained pre-coated boron film is 170nm (= 255(a.u) × 2/3). Since the thickness of pre-coated boron film was 350nm, the net erosion depth is 350nm－170nm = 180nm. After the 10th experimental campaign, the probes were removed from the vacuum chamber wall, and the depth profile of atomic composition and the retained amounts of discharge gases were investigated by AES with 3 keV Ar+ sputtering and TDS, respectively.

3. Results and discussion

3.1. Characteristics of deposition layer

Major species deposited on the probe were carbon, boron, oxygen and iron. Figure 3 shows the thickness of deposited boron and carbon film of each sector. The carbon was deposited on the top surface of all probes as shown in Fig.2 (a) and (b). The thickness of boron film in toroidal direction depends on the positions of GDC anode and nozzle in LHD.

3.2. Toroidal dependence of eroded depth

Fig. 4 shows the eroded depth of pre-coated boron film in each toroidal sector. The strong erosion of boron film

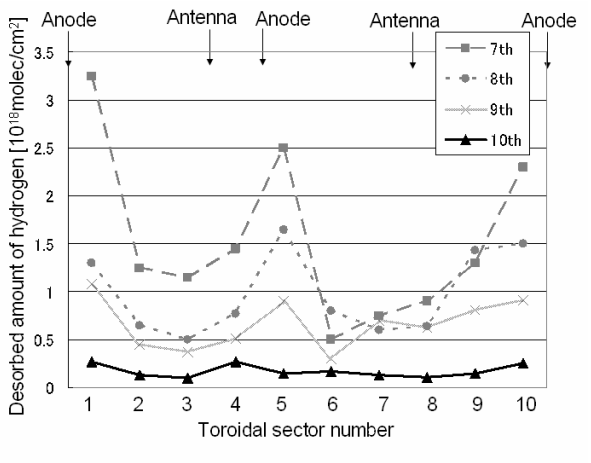

Fig.5 Comparison of retained amounts of hydrogen in stainless steel samples placed at the lower first wall along the toroidal direction through 7th~10th campaign.

was observed in the probes at sectors 1, 4, 5, 6, 10. The pre-coated boron film at 3 sector (250nm) and 5 sector (550 nm) was entirely eroded. And in fig.4 the arrow at sector 3 and sector 5 means the actual eroded depth was larger than the 250nm (sector 3) and 550nm (sector5). These results indicate that the wall erosion was mainly caused by the glow discharges, and the erosion depth by the glow discharge depended on the distance from the anodes.

3.3. Toroidal distribution of hydrogen retention

Figure 5 also shows the comparison of retained amounts of hydrogen in stainless steel probes placed along the toroidal direction through 7-10th campaigns. In Fig.5, the positions of two anodes and two ICRF antennas are also shown. The amount of retained hydrogen was large near the anodes through all campaign. This indicates that hydrogen implantation is mainly caused by glow discharge. It suggests the contribution of the current density of the glow discharge to the erosion. In addition, it was found that the retained amount of hydrogen is decreasing campaign by campaign. This might result from the reduction of hydrogen glow discharge time (7th:700h, 8th:500h, 9th: 290h, 10th: 250h) and the increase of helium glow discharge cleaning time (7th:100h, 8th:100h, 9th: 240h, 10th: 400h).

3.4 Amount of retained helium

In previous works, the retained helium in the stainless steel desorbed mainly in the temperature region higher than 800-900 K for the sample exposed to only helium main discharges, while the amount of helium desorbed in the temperature region lower than 900K is large for the sample exposed to only the glow discharges [8]. In Fig.6, thermal desorption spectra of helium from SS316L sample in sector 5 and 8 are shown.

In Fig.7, the total amount of helium in the 10th

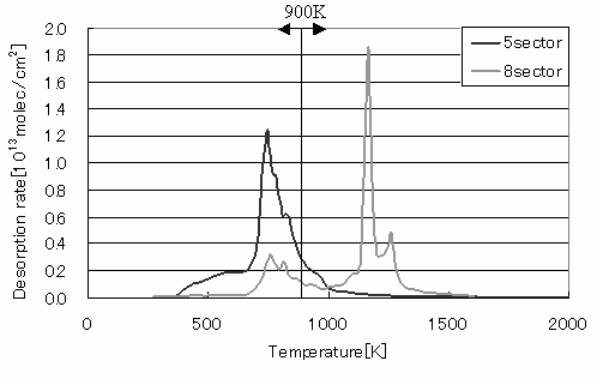

Fig.6 Thermal desorption spectra of helium for the probe located at 5 sector (close to anode) and 8 sector (close to antenna).

experimental campaign and the case of subtracted this amount up to 900K and above 900K are also shown. Typically helium plasma discharges were supported by ICRF heating systems. The data without ICRF heating in the 7th experimental campaign (2003-2004) are also shown in Fig. 8 as a reference. The amount of helium desorbed up to 900 K was large near glow anodes in the 7th and 10th experimental campaigns. Since the anode voltage during glow discharges was several hundreds eV, the helium ions were retained in the shallow depth region of several nm. On the other hand, the amount of helium desorbed above 900 K was large near the ICRF antenna in the 10th experimental campaign only. The sample exposed to main plasma discharges was influenced by high energy helium ion with several keV accelerated by ICRF antenna. In this case, the implantation depth of helium ions was 10-20 nm, so the helium might desorbed above 900 K. But in the case of main discharges without ICRF heating, theamount of helium desorbed above 900 K was not large near the ICRF antenna. This result indicates that ICRF heating has a large influence to an implantation mechanism of helium. From the results in Figs. 7 and 8, helium implantation was caused by both glow discharge and main discharge in LHD.

4. Conclusion

For an understanding the characteristics of deposition /erosion rate on toroidal direction, pre-coated samples are used in LHD. The major species of deposits on the top surface was carbon. The erosion rate is analyzed using pre-coated boron film with known thickness and then toroidal dependence of erosion is shown experimentally. The wall erosion clearly depends on the distance from anodes. Especially, the sample probe at sector 5 was strongly eroded and all pre-coated film (550nm) disappeared.

The amount of retained hydrogen was large near the anodes, and hydrogen implantations to the first wall mainly occur during glow discharges. The desorbed amount of helium in lower temperature region (up to 900K), was large near the anodes. On the other hand, in higher temperature region (above 900K), the amount was

E-mail address: yagiha@pop.qe.eng.hokudai.ac.jp

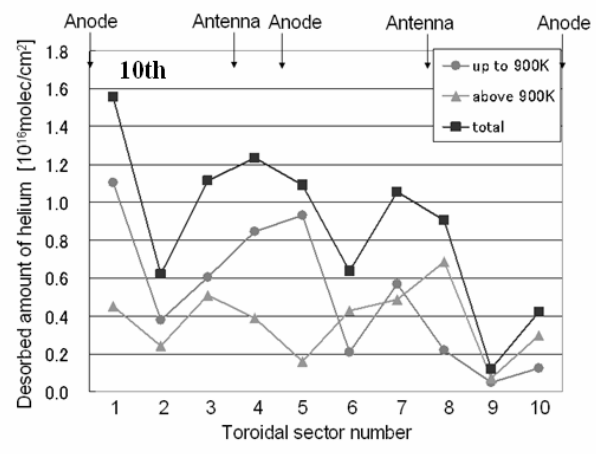

Fig.7 Desorbed amount of helium, *up to 900K*, *above 900K*, and total amount as the case of plasma discharges with ICRF heating systems in 10th experimental campaign.

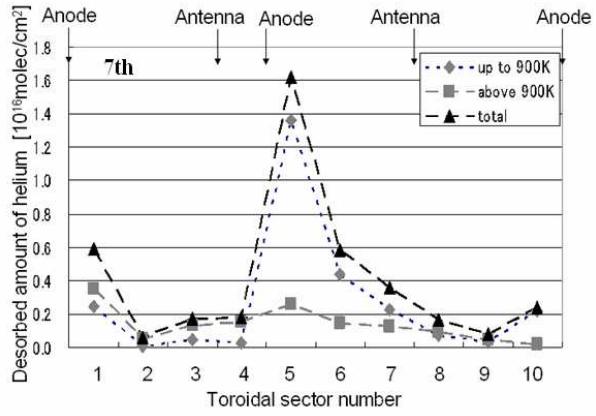

Fig.8 Desorbed amount of helium, *up to 900K*, *above 900K*, and total amount as the case of plasma discharges without ICRF heating systems in 7th experimental campaign.

large near the ICRF antennas. This result indicates the influence by high-energy helium ions heated by ICRF heating. The total amount of desorbed helium was large both near anodes and antennae. This indicates that helium implantation was caused by both glow discharge and main discharge.

5. Acknowledgements

This work was supported by the NIFS Collaboration Research (NIFS06KLPP301), and partly by the JSPS CUP Core University Program in the field of plasma and nuclear fusion.

References

[1] K.Nishimura, N.Ashikawa, S. Masuzaki, J. Miyazawa, A. Sagara et al, J. Nucl. Mater. 337-339 (2005) 431.

E-mail address: yagiha@pop.qe.eng.hokudai.ac.jp

[2] N. Ashikawa, K. Kizu, J. Yagyu, T. Nakahata, Y. Nobuta et al, J. Nucl. Mater. 363-365 (2007) 1352.
[3] A. Sagara, N. Inoue, N. Noda, O. Motojima, et al., J. Plasma Fusion Res. 75 (1999) 263.
[4] T. Hino, T. Ohuchi, M. Hashiba, Y. Yamauchi, Y. Hirohata, N. Inoue, A. Sagara, N. Noda, O. Motojima, J. Nucl. Mater. 290–293 (2001) 1176.
[5] S. Masuzaki, K. Akaishi, H. Funaba, M. Goto, K. Ida, et al.,J. Nucl. Mater. 290–293 (2001) 12
[6]T. Hino, Y. Nobuta , N. Ashikawa , K. Nishimura , S. Masuzaki, J. Nucl. Mater. 82 (2007) 1621–1626
[7] T. Mutoh, R. Kumazawa, T. Seki, K. Saito, T. Watari and Y. Torii et al., Nucl. Fusion 43 (2003) 738–743.
[8] Y. Nobuta, Y. Yamauchi, Y. Hirohata, T. Hino, N. Ashikawa, J. Nucl. Mater. 337-339(2005)932-936